

Atomic motion and density fluctuations in cavity QED with atomic beams

L. Horvath and H. J. Carmichael

University of Auckland, Private Bag 92019, Auckland, New Zealand

ABSTRACT

Ab initio quantum trajectory simulations of a cavity QED system comprising an atomic beam traversing a coherently driven standing-wave cavity are carried out. The intensity correlation function in transmission is computed and compared with the experimental measurements of Rempe *et al.* [Phys. Rev. Lett. **67**, 1727 (1991)] and Foster *et al.* [Phys. Rev. A **61**, 053821 (2000)]. It is shown that atomic beam density fluctuations induced by the motion of the atoms can account for the reported disagreement of the experimental results with theory (by an overall scale factor of 2 to 4). Moderate misalignments of the atomic beam produce large intracavity photon number fluctuations which significantly degrade the quantum correlations. One parameter fits to the experimental data are made in the weak-field limit with the adjustable parameter being the atomic beam tilt. Departures of the experimental conditions from the weak-field limit are discussed.

Keywords: Cavity QED, photon antibunching, quantum fluctuations, quantum trajectory theory.

1. INTRODUCTION

Atom-cavity systems have been studied extensively, first to explore the differences between classical and quantum phenomena and also for their possible application in quantum information science. To observe their quantum fluctuations in the optical regime, experimental measurements of the intensity correlation function¹⁻⁴ and conditional homodyne correlations⁵⁻⁷ have been performed. Such measurements reveal various features of cavity QED dynamics, e.g., the so-called vacuum Rabi oscillation.^{8,9} More importantly, nonclassical correlations are observed, providing unequivocal evidence of quantum field effects in cavity QED.¹⁰⁻¹³

Most such experiments use thermal atomic beams¹⁻³ and accurately modeling these experiments is a challenging task. The atomic beam typically carries hundreds of atoms into the interaction volume. Thus, the theoretical description is contained within an enormous Hilbert space; the Hilbert space grows and shrinks with the number of atoms, which inevitably fluctuates over time, and the atoms traverse a spatially varying cavity mode so their coupling strengths change in time. A realistic model must take all of these effects into account. Considering the weak-field limit, a minimal truncation of the Hilbert space at the two-quanta level may be made. If the atomic motion is then neglected, relatively simple analytic formulas can be derived,^{10,12} including, most generally, different coupling strengths for different atoms.¹ Such weak-field formulas that neglect atomic motion form the basis of all previous comparisons of theory with experimental results.^{1,3,14}

Despite the popularity and qualitative correctness of these formulas, a persistent quantitative discrepancy with the measurements remains unexplained. The first experimental results were slightly shifted and the amplitude of the Rabi oscillation scaled down by a factor of 4 in order to achieve reasonable agreement with the theory;¹ scaling down by a factor of more than 2 is needed for more recent data sets³ (see Fig. 1). While Foster *et al.*³ achieved a reasonable fit by introducing detunings into the theory to account for Doppler broadening, it is questionable whether their procedure accurately represents the conditions in a standing-wave cavity.

In this paper we attempt to explain the persistent disagreement between theory and experiment by including the one feature omitted by the previous theoretical treatment: the motion of the atoms and the atomic beam density fluctuations induced by that motion. In this regard, any misalignment of the atomic beam from perpendicular to the cavity axis is of paramount importance, since it gives rise to atomic motion through the standing

Further author information:

E-mail: h.carmichael@auckland.ac.nz, Tel: +64 9 373 7599 ext 88899, Fax: +64 9 373 7445

wave—an amplitude modulation of the dipole coupling strength. For misalignments on the order of 10 mrad a significant enhancement of the background fluctuations of the intracavity photon number can result. We propose this as a feasible mechanism underlying the observed degradation of the quantum correlations. In support of the proposal we report excellent fits to the experimental data obtained from *ab initio* quantum trajectory simulations made with only one adjustable parameter, the tilt of the atomic beam.

We present our physical model and review the weak-field theory without atomic motion in Sec. 2. The quantum trajectory treatment including atomic motion is introduced in Sec. 3. Here we demonstrate the importance of density fluctuations by calculating semiclassical intensity correlation functions that include the effects of atomic motion but omit the quantum jump that accompanies each photon detection in the full quantum calculation. We show that in the presence of a moderate atomic beam tilt the internal system state fails to follow the density fluctuations adiabatically, which contributes significantly to the degradation of the quantum correlations.

The results of full *ab initio* quantum trajectory simulations are presented in Sec. 4. Best one parameter fits to sample data sets from the experiments of Rempe *et al.*¹ and Foster *et al.*³ are shown. Good agreement is obtained in the former case, and excellent in the latter, using atomic beam tilts on the order of 10 mrad. The simulations are carried out in the weak-field limit using a two-quanta truncation of the Hilbert space (approximately 20,000 equations for 200 atoms).

Based on the photon counting rates reported, the experiments are carried out in the vicinity of, but strictly outside, the weak-field regime. Spontaneous emission is then an important consideration since the two-quanta truncation of the quantum trajectory equations assumes that no emissions, either spontaneous or from the cavity, other than the “start” and “stop” emissions triggering the time-to-digital converters, occur within a few correlation times of any “start”. It would appear that this is not true in the experiments. Spontaneous emissions do occur; for strong coupling and weak excitation, they are far more likely than emission from the cavity. This requires the quantum trajectory equations to take into account sequences of three or more quantum jumps, for which a minimal truncation of the Hilbert space at three or more quanta is needed. We present results in Sec. 4 based on a three-quanta truncation (approximately 1,000,000 equations for 200 atoms). They are consistent with the photon counting rates reported by Rempe *et al.*¹ but the intensity correlation function is significantly altered at the count rates reported by Foster *et al.*³ Our conclusions are presented in Sec. 5.

2. MODEL AND REVIEW

Atomic beams provide a convenient means of delivering atoms into an interaction volume. They have been used extensively for experiments in cavity QED at both optical and microwave frequencies. Typically, the beam is generated from an atomic vapor produced in a small oven, from which atoms escape via a collimated opening. Atoms exit the oven at some average rate, but otherwise in a random fashion, with speeds governed by the Maxwell-Boltzmann distribution modified by a velocity factor to account for the likelihood of escape. Thus, experiments have control over the mean density, average speed, and direction of the atomic beam, but not over the exact number of atoms in the interaction volume, or the speeds and locations of the atoms. Fluctuations in the number and locations of the atoms are rather easily taken into account, and were included in the earliest comparisons of measured intensity correlation functions with theory.¹ The role of atomic motion is not so easily discerned.

Atomic beam fluctuations are particularly significant at low densities.¹⁵ The densities of concern to us are quite high, characterized by the parameter $\bar{N}_{\text{eff}} = 18$ in the experiment of Rempe *et al.*¹⁶ and $\bar{N}_{\text{eff}} = 13$ in the experiment of Foster *et al.*,¹⁷ where \bar{N}_{eff} is the average number of atoms located within the cavity mode waist. Although the number of atoms contributing to the interaction is larger than \bar{N}_{eff} by approximately a factor of ten,¹⁵ and therefore on the order of 150 atoms, we find, nevertheless, that fluctuations of the atomic density produce fluctuations of the intracavity photon number that are far larger than the quantum fluctuations to be measured. The reason for this is the atomic motion; in particular the fact that this motion is not slow compared to the time scales governing the internal cavity QED dynamics (vacuum-Rabi frequency and damping rates). Fast moving density fluctuations excite vacuum Rabi oscillations, but with a classical (bunched) rather than nonclassical (antibunched) signature in the intensity correlation function. Significant degradation of the measured quantum correlations results. We model this behavior on the basis of a master equation that includes the motion of each atom parametrically.

2.1. Master Equation for Cavity QED with Atomic Beams

We consider a collimated atomic beam traversing a standing-wave cavity, driven coherently at the resonant frequency of the TEM₀₀ mode. At time t there are $N(t)$ atoms within the interaction volume, which we define by¹⁵

$$V_F \equiv \{(x, y, z) : g(x, y, z) \geq F g_{\max}\}, \quad (1)$$

with cut-off parameter $F < 1$ and

$$g(x, y, z) = g_{\max} \cos(kz) \exp[-(x^2 + y^2)/w_0^2], \quad (2)$$

where g_{\max} is the atomic dipole coupling constant at an antinode of the cavity mode, $k = 2\pi/\lambda$ is the wavenumber, λ the resonant wavelength, and w_0 is the cavity mode waist. The $N(t)$ two-state atoms are resonant with the cavity field, and the atom-cavity interaction is described by the master equation in the interaction picture

$$\begin{aligned} \dot{\rho} = & \mathcal{E}[\hat{a}^\dagger - \hat{a}, \rho] + \sum_{j=1}^{N(t)} g(\mathbf{r}_j(t)) [\hat{a}^\dagger \hat{\sigma}_{j-} - \hat{a} \hat{\sigma}_{j+}, \rho] \\ & + \kappa (2\hat{a}\rho\hat{a}^\dagger - \hat{a}^\dagger\hat{a}\rho - \rho\hat{a}^\dagger\hat{a}) + \frac{\gamma}{2} \sum_{j=1}^{N(t)} (2\hat{\sigma}_{j-}\rho\hat{\sigma}_{j+} - \hat{\sigma}_{j+}\hat{\sigma}_{j-}\rho - \rho\hat{\sigma}_{j+}\hat{\sigma}_{j-}), \end{aligned} \quad (3)$$

where $\mathbf{r}_j(t)$ is the location of atom j , \mathcal{E} is the strength of the external field, γ is spontaneous emission rate, κ is the damping rate of the cavity field, \hat{a}^\dagger and \hat{a} are creation and annihilation operators for the cavity mode, and $\hat{\sigma}_{j+}$ and $\hat{\sigma}_{j-}$ are creation and annihilation operators for atom j . Both $N(t)$ and $\{\mathbf{r}_j(t); j = 1, \dots, N(t)\}$ are changing in time in accord with the stochastic model set out in Sec. 3.1.

2.2. Weak-field Formula without Atomic Motion

The implementation of our model, even as a quantum trajectory simulation, faces serious technical difficulties due to the enormous size of the Hilbert space. We anticipate that for $\bar{N}_{\text{eff}} = 18$ and $F = 0.1$ the number of atoms in the interaction volume commonly exceeds $N(t) = 200$; in fact, for the simulations reported in Sec. 4.1 a cut-off $F = 0.01$ was used and $N(t)$ commonly exceeded 400 atoms. The solution to this problem is to truncate the Hilbert space at the two-quanta level, the minimum permitted if two-photon correlations are to be addressed. The truncation may be justified by expanding the density matrix in powers of \mathcal{E}/κ ;^{18,19} to dominant order, the density matrix may be factorized as a pure state $\rho = |\psi\rangle\langle\psi|$.^{10,12}

The physical basis of this weak-field approximation is made clear by a quantum trajectory unraveling of the master equation dynamics. If we assume that for a few correlation times before and after a ‘‘first’’ photon emission from the cavity (the ‘‘start’’ to the time-to-digital converters) there are no spontaneous emissions or further cavity emissions, then the quantum state is determined by the between-jump evolution only; thus, it is pure and satisfies the standard non-unitary Schrödinger equation [Eq. (22)]. The weak-field approximation is therefore justified so long as the scattered photon flux is much less than the inverse of the intensity correlation time. It allows us to write the conditional system state as

$$|\psi_{\text{REC}}(t)\rangle = |00\rangle + \alpha(t)|10\rangle + \sum_{j=1}^N \beta_j(t)|0j\rangle + \eta(t)|20\rangle + \sum_{j=1}^N \zeta_j(t)|1j\rangle + \sum_{j>k=1}^N \vartheta_{jk}(t)|0jk\rangle, \quad (4)$$

where $|00\rangle$ is the ground state (no photons in the cavity and no atoms excited), $|n0\rangle$ has n photons in the cavity and no atoms excited, $|1j\rangle$ is the two-quanta state with one photon in the cavity and the j^{th} atom excited, and $|0jk\rangle$ is the two-quanta state with no photons in the cavity and the j^{th} and k^{th} atoms excited. Neglecting the atomic motion and considering a fixed spatial configuration $\{\mathbf{r}_j\}$ of N atoms, the intensity correlation function obtained from Eqs. (3) and (4) is^{1,10}

$$g_{\{\mathbf{r}_j\}}^{(2)}(\tau) = \left\{ 1 - \frac{[1 + \xi(1 + C_{\{\mathbf{r}_j\}})]S_{\{\mathbf{r}_j\}} - 2C_{\{\mathbf{r}_j\}}}{1 + (1 + \xi/2)S_{\{\mathbf{r}_j\}}} e^{-\frac{1}{2}(\kappa + \gamma/2)\tau} \left[\cos(\Omega_{\{\mathbf{r}_j\}}\tau) + \frac{\frac{1}{2}(\kappa + \gamma/2)}{\Omega_{\{\mathbf{r}_j\}}} \sin(\Omega_{\{\mathbf{r}_j\}}\tau) \right] \right\}^2, \quad (5)$$

with vacuum Rabi frequency

$$\Omega_{\{\mathbf{r}_j\}} = \sqrt{N_{\text{eff}}^{\{\mathbf{r}_j\}} g_{\text{max}}^2 - \frac{1}{4}(\kappa - \gamma/2)^2}, \quad (6)$$

effective number of atoms in the interaction volume

$$N_{\text{eff}}^{\{\mathbf{r}_j\}} = \sum_{j=1}^N g^2(\mathbf{r}_j) / g_{\text{max}}^2, \quad (7)$$

and

$$S_{\{\mathbf{r}_j\}} \equiv \sum_{j=1}^N \frac{2C_{1j}}{1 + \xi(1 + C_{\{\mathbf{r}_j\}}) - 2\xi C_{1j}}, \quad (8)$$

where we define

$$C_{\{\mathbf{r}_j\}} \equiv \sum_{j=1}^N C_{1j}, \quad C_{1j} \equiv g^2(\mathbf{r}_j) / \kappa\gamma, \quad \xi \equiv 2\kappa/\gamma. \quad (9)$$

In reality the configuration $\{\mathbf{r}_j(t)\}$ and number of atoms $N(t)$ are both functions of time. Atoms are delivered to the interaction volume by the atomic beam at mean density¹⁵

$$\varrho = 4\bar{N}_{\text{eff}} / \pi w_0^2 l, \quad \bar{N}_{\text{eff}} = \overline{N_{\text{eff}}^{\{\mathbf{r}_j\}}}, \quad (10)$$

where l is the atomic beam width and the overbar denotes the ensemble average over configurations and number of atoms. Previously it has been assumed that the average speed of the atoms is sufficiently low for the system state to adiabatically follow the spatial configuration. Under this assumption, the intensity correlation function is written as the ensemble average²⁰

$$g^{(2)}(\tau) = \frac{\overline{\langle \hat{a}^\dagger(0) \hat{a}^\dagger(\tau) \hat{a}(\tau) \hat{a}(0) \rangle_{\{\mathbf{r}_j\}}}}{\left(\overline{\langle \hat{a}^\dagger \hat{a} \rangle_{\{\mathbf{r}_j\}}} \right)^2}, \quad (11)$$

or in terms of the normalized correlation function (5),

$$g^{(2)}(\tau) = \frac{\overline{\left(\langle \hat{a}^\dagger \hat{a} \rangle_{\{\mathbf{r}_j\}} \right)^2 g_{\{\mathbf{r}_j\}}^{(2)}(\tau)}}{\left(\overline{\langle \hat{a}^\dagger \hat{a} \rangle_{\{\mathbf{r}_j\}}} \right)^2}, \quad (12)$$

with mean photon number under the two-quanta truncation¹⁰

$$\langle \hat{a}^\dagger \hat{a} \rangle_{\{\mathbf{r}_j\}} = \left(\frac{\mathcal{E}/\kappa}{1 + 2C_{\{\mathbf{r}_j\}}} \right)^2. \quad (13)$$

Figure 1 compares the intensity correlation function obtained from Eq. (12) with two experimental data sets, one each from the experiments of Rempe *et al.*¹ and Foster *et al.*³ These experimental results and the parameters under which they were obtained (see the captions to Figs. 2 and 3) are adopted for all future comparison between experiment and theory. With the atomic motion neglected, the main disagreement is the smaller amplitude of the measured vacuum Rabi oscillation. It is smaller by a factor of 4 in Fig. 1(a), as the authors of the original publication noted,¹ and by a factor of a little more than 2 in Fig. 1(b); there is also a significant difference of shape near the origin in Fig. 1(b). Though a smaller effect, note also that neither the experimental result nor the theoretical curve appears to be asymptotic to $g^{(2)}(\infty) = 1$ in Fig. 1(a); the same is true for the theoretical curve in Fig. 1(b). Here is the only hint of the significant role of atomic beam density fluctuations. The approximation made by Eq. (11) gives these fluctuations an infinite correlation time, and for this reason the correlation function is not asymptotic to $g^{(2)}(\infty) = 1$.²⁰ The deviation of the asymptote from unity is rather small; but as we show in Secs. 3 and 4, the density fluctuations are the cause of the loss of vacuum Rabi amplitude as well.

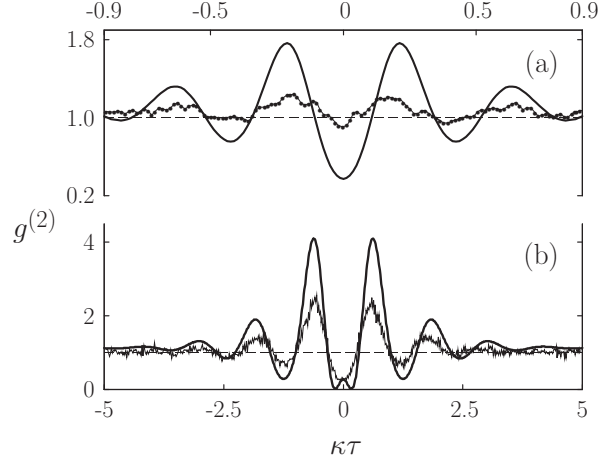


Figure 1. Comparison of the intensity correlation function computed from the two-quanta truncation without atomic motion [Eq. (12)] and the experimental measurements of Rempe *et al.*¹⁶ (a) and Foster *et al.*¹⁷ (b). The parameters are: (a) $\bar{N}_{\text{eff}} = 18$, $g_{\text{max}}/\kappa = 3.56$, and $\gamma/\kappa = 5.56$; (b) $\bar{N}_{\text{eff}} = 13$, $g_{\text{max}}/\kappa = 1.47$, and $\gamma/\kappa = 0.77$.

3. DENSITY FLUCTUATIONS AND ATOMIC MOTION

In this section we demonstrate the importance of atomic beam density fluctuations and atomic motion by isolating these effects from the quantum fluctuations. We implement the model from Sec. 2.1 as a quantum trajectory simulation and calculate the semiclassical correlation function

$$g_{\text{sc}}^{(2)}(\tau) = \frac{\overline{\langle(\hat{a}^\dagger\hat{a})(t_k)\rangle_{\text{REC}}\langle(\hat{a}^\dagger\hat{a})(t_k+\tau)\rangle_{\text{REC}}}}{\left(\overline{\langle(\hat{a}^\dagger\hat{a})(t_l)\rangle_{\text{REC}}}\right)^2}, \quad (14)$$

where $\langle(\hat{a}^\dagger\hat{a})(t)\rangle_{\text{REC}}$ is the conditional photon number expectation, and the overbar denotes the average over a set of sample times t_k (t_l). Note that Eq. (14) introduces no quantum jump at the times t_k ; these times are not specifically the times of photon emission from the cavity. Thus, we omit the quantum fluctuations associated with the backreaction from the detection of photons, but include the effects of atomic beam density fluctuations. We compute the correlation function (14) from the full simulation of $\langle(\hat{a}^\dagger\hat{a})(t)\rangle_{\text{REC}}$, including the internal system dynamics, and also from the adiabatic approximation

$$\langle(\hat{a}^\dagger\hat{a})(t)\rangle_{\text{REC}} = \left(\frac{\mathcal{E}/\kappa}{1+2C_{\{\mathbf{r}_j(t)\}}}\right)^2, \quad (15)$$

where $\{\mathbf{r}_j(t)\}$ is the time-dependent configuration of atoms in the interaction volume. Correlation functions are computed for an atomic beam aligned perpendicular to the cavity axis and for a beam with a tilt.

3.1. Quantum Trajectory Equations

Our numerical method simulates an atomic beam undergoing classical motion that runs in parallel with a quantum trajectory simulation for the system quantum state. We first summarize our model for the atomic beam.

Applying the theory of effusive sources to a thin-walled orifice, we assume a Maxwell-Boltzmann distribution of atomic velocities inside the source of the atomic beam, with average speed

$$\bar{v}_{\text{source}} = \sqrt{8k_B T/\pi M}, \quad (16)$$

where T is the source temperature and M is the atomic mass. To realize the density (10) corresponding to a given \bar{N}_{eff} , atoms are created randomly at the source output—on the plane $x = -w_0\sqrt{|\ln F|}$ in the simulations—at the rate

$$R_{\text{atom}} = 64\bar{N}_{\text{eff}}\bar{v}_{\text{beam}}/3\pi^2w_0, \quad (17)$$

where

$$\bar{v}_{\text{beam}} = \sqrt{9\pi k_B T / 8M} = (3\pi/8)\bar{v}_{\text{source}} \quad (18)$$

is the average speed of an atom in the atomic beam. At its creation, creation time t_0^j , the j^{th} atom is assigned a random position and velocity, with

$$\mathbf{r}_j(t_0^j) = \left(-w_0\sqrt{|\ln F|}, y_j(t_0^j), z_j(t_0^j) \right) \quad (19)$$

and

$$\mathbf{v}_j = v_j (\cos \theta, 0, \sin \theta), \quad (20)$$

where θ is the tilt of the atomic beam, $y_j(t_0^j)$ and $z_j(t_0^j)$ are random variables uniformly distributed over the intervals $|y_j(t_0^j)| \leq w_0\sqrt{|\ln F|}$ and $|z_j(t_0^j)| \leq \lambda/4$, and v_j has probability distribution

$$P(v_j)dv_j = 2u^3(v_j)e^{-u^2(v_j)} du(v_j), \quad u(v_j) \equiv 2v_j/\sqrt{\pi}\bar{v}_{\text{source}}. \quad (21)$$

Subsequently, each atom moves freely across the cavity, passing out of the interaction volume when it reaches the plane $x_j(t) = w_0\sqrt{|\ln F|}$; the atomic beam density is assumed low enough that collisions may be overlooked. Atoms are created in the ground state and return to the ground state (are disentangled) on exiting the interaction volume. The latter may be achieved by spontaneous emission or without it, the choice made by a random number and the probability for the atom to be in the excited state (effectively a measurement of the internal atomic state is performed).

The quantum trajectory simulation is based upon the direct photoelectron counting unraveling of master equation (3).^{21–23} The system state is expanded in the two-quanta basis [Eq. (4)] with a basis size that grows and shrinks with $N(t)$. The between-jump evolution of the (unnormalized) conditional state satisfies the nonunitary Schrödinger equation

$$\frac{d|\bar{\psi}_{\text{REC}}\rangle}{dt} = \frac{1}{i\hbar}\hat{H}_B(t)|\bar{\psi}_{\text{REC}}\rangle, \quad (22)$$

with non-Hermitian Hamiltonian

$$\hat{H}_B(t)/i\hbar = \mathcal{E}(\hat{a}^\dagger - \hat{a}) + \sum_{j=1}^{N(t)} g(\mathbf{r}_j(t))(\hat{a}^\dagger \hat{\sigma}_{j-} - \hat{a} \hat{\sigma}_{j+}) - \kappa \hat{a}^\dagger \hat{a} - \frac{\gamma}{2} \sum_{j=1}^{N(t)} \hat{\sigma}_{j+} \hat{\sigma}_{j-}. \quad (23)$$

It is interrupted by quantum jumps,

$$|\bar{\psi}_{\text{REC}}\rangle \rightarrow \hat{a}|\bar{\psi}_{\text{REC}}\rangle, \quad (24)$$

and

$$|\bar{\psi}_{\text{REC}}\rangle \rightarrow \hat{\sigma}_{j-}|\bar{\psi}_{\text{REC}}\rangle, \quad j = 1, \dots, N(t), \quad (25)$$

which occur at the rates $2\kappa\langle\hat{a}^\dagger\hat{a}\rangle_{\text{REC}}$ and $\gamma\langle\hat{\sigma}_{j+}\hat{\sigma}_{j-}\rangle_{\text{REC}}$, $j = 1, \dots, N(t)$, respectively. In the weak-field limit, all jump rates are very small, such that the evolution under Eq. (22) continues uninterrupted most of the time—this, again, is the justification for the pure state factorization of the density matrix argued for in Sec. 2.2. Note that the non-Hermitian Hamiltonian (23) is explicitly time dependent and stochastic, due to its dependence on the Monte-Carlo simulation of the atomic beam.

3.2. Semiclassical Intensity Correlations

For an atomic beam aligned perpendicular to the cavity axis, the dipole coupling constants $g(\mathbf{r}_j(t))$ change in time due to motion through the Gaussian transverse profile of the cavity mode only. We may characterize the rate of change by the cavity mode transit time, determined from the mean speed of the atoms and the cavity mode waist. In the experiment of Rempe *et al.*¹⁶ the transit time is $w_0/\bar{v}_{\text{source}} = 182\text{nsec}$, compared with a decay time for the vacuum Rabi oscillation of $2(\kappa + \gamma/2)^{-1} = 94\text{nsec}$. The corresponding numbers in the Foster *et al.*¹⁷ experiment are $w_0/\bar{v}_{\text{source}} = 66\text{nsec}$ and $2(\kappa + \gamma/2)^{-1} = 29\text{nsec}$. The ratio in both cases is approximately 2; thus, an approximate adiabatic following of the atomic beam density fluctuations might be expected. Figures 2(a) and 3(a) show examples of the fluctuations in photon number induced by the fluctuations of the atomic beam.

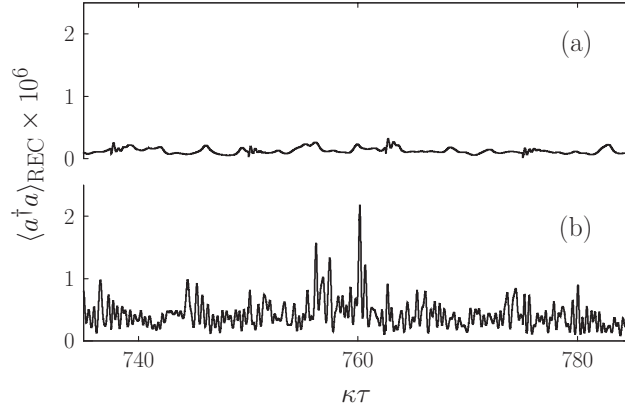


Figure 2. Typical trajectory of the intracavity photon number expectation with (a) no tilt of the atomic beam and (b) an atomic beam tilt of 9.6mrad; for the parameters of Rempe *et al.*¹⁶: $\bar{N}_{\text{eff}} = 18$, $\kappa/2\pi = 0.9\text{MHz}$, $g_{\text{max}}/\kappa = 3.56$, $\gamma/\kappa = 5.56$, $w_0 = 50\mu\text{m}$, $\lambda = 852\text{nm}$, and $\bar{v}_{\text{beam}} = 323.4\text{m/s}$. The driving field strength is $\mathcal{E}/\kappa = 2.5 \times 10^{-2}$. Cavity emissions are imposed in accord with the sampling scheme described in Sec. 4.

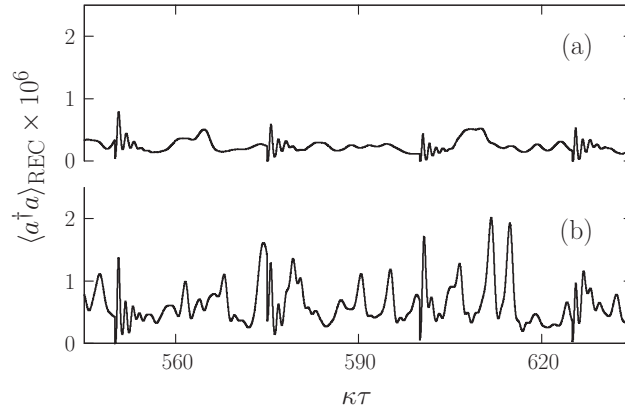


Figure 3. As in Fig. 2 but for the parameters of Foster *et al.*¹⁷: $\bar{N}_{\text{eff}} = 13$, $\kappa/2\pi = 7.9\text{MHz}$, $g_{\text{max}}/\kappa = 1.47$, $\gamma/\kappa = 0.77$, $w_0 = 21.5\mu\text{m}$, $\lambda = 780\text{nm}$, and $\bar{v}_{\text{beam}} = 384.5\text{m/s}$.

The ringing at regular intervals along these curves is the transient response to *enforced* cavity-mode quantum jumps [Eq. (24)] introduced to sample the quantum fluctuations (see Sec. 4). Ignoring the forced jumps for the present, as anticipated the fluctuations induced by the atomic beam are significantly slower than the vacuum Rabi oscillation and occur on a similar time scale to the vacuum Rabi oscillation decay.

Figures 2(b) and 3(b) introduce a tilt of the atomic beam away from perpendicular to the cavity axis. Rempe *et al.*¹ do not comment on the tilt that might reasonably be present in their experiment, but Foster *et al.*³ speak of tilts as large as 1° (17.45mrad). We use approximately half that value for the figures. The tilt brings significant changes to the background fluctuations. They increase in amplitude, though by less than it might appear from the figures. A numerically computed probability distribution over photon number shows an increase in variance (relative to the square of the mean) by a factor of 2.25 in Fig. 2 and 1.45 in Fig. 3. The distribution is asymmetric, however, with a long tail of fluctuations above the mean, which consequently falls above the most probable photon number. The asymmetry is accentuated by the tilt.

More important is the increase in the frequency of the fluctuations, where again, the biggest change occurs in the Rempe *et al.*¹ experiment. In Fig. 2(b) the background fluctuations now have a frequency similar to that of the vacuum Rabi oscillation, and from the combination of the increase in amplitude and frequency, the enforced quantum jumps are completely lost in the classical background fluctuations caused by the atomic beam.

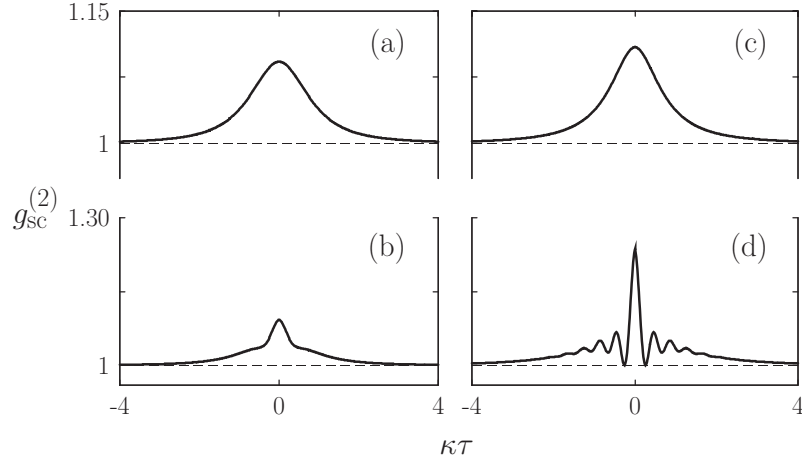


Figure 4. Semiclassical intensity correlation functions assuming adiabatic following of the intracavity photon number expectation (left column) and without adiabatic following (right column), with no tilt of the atomic beam [(a) and (c)] and an atomic beam tilt of 9.0mrad [(b) and (d)]; for the parameters of Rempe *et al.*¹⁶ given in Fig. 2.

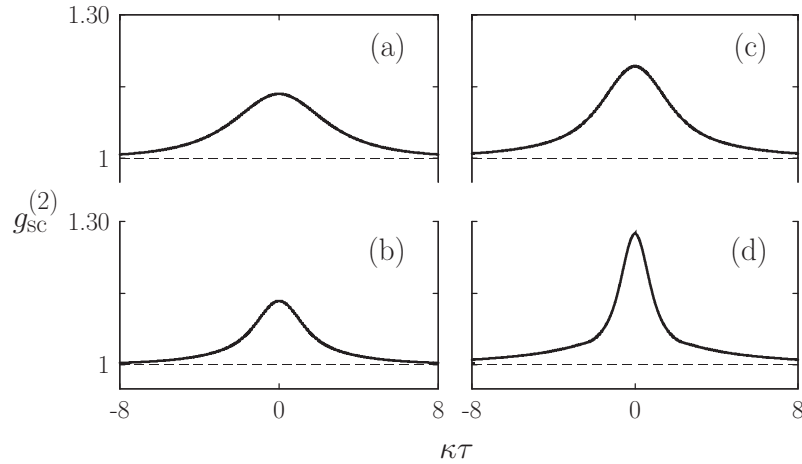


Figure 5. As in Fig. 4 but with an atomic beam tilt of 10mrad [(b) and (d)] and for the parameters of Foster *et al.*¹⁷ given in Fig. 3.

For a quantitative characterization of these fluctuations, we carried out a quantum trajectory simulation truncated at the one-quantum level and computed the semiclassical correlation function (14). Results for the two experiments are displayed in Figs. 4 and 5. In each case, the correlation functions shown to the left were obtained by assuming the photon number fluctuations adiabatically follow the fluctuations of the atomic beam [Eq. (15)], while those shown to the right were obtained without the adiabatic approximation. The upper curves [(a) and (c)] hold for an atomic beam aligned perpendicular to the cavity axis and the lower [(b) and (d)] for tilted atomic beams.

A number of comments are in order. Considering first the results for a perfectly aligned atomic beam, the correlation times are given approximately by the quoted transit times: 191nsec and 167nsec from Figs. 4(a) and (c), respectively, compared with $w_0/\bar{v}_{\text{source}} = 182\text{nsec}$; and from Figs. 5(a) and (c), 68nsec and 53nsec, respectively, compared with $w_0/\bar{v}_{\text{source}} = 66\text{nsec}$. As these numbers show, there is a small decrease in the correlation time due to the nonadiabatic response of the photon number to the atomic beam fluctuations—by approximately 10-20%. Along with it there is a small increase in the fluctuation amplitude.

Considering then the tilted atomic beam, there is significant change, most evident in frame (d) of each figure. There is first an increase in the size of the fluctuations—the factors 2.25 and 1.45 noted above. More significant, however, is the apparent decomposition of the correlation function into two distinct pieces: a central component with short correlation time and a much broader component with correlation time larger than $w_0/\bar{v}_{\text{source}}$. In the presence of the atomic beam tilt, the dynamics are notably nonadiabatic. There is now a velocity component in the direction of the standing wave, with transit times through a quarter wavelength of $\lambda/4\bar{v}_{\text{source}} \sin \theta = 86 \text{ nsec}$ for the Rempe *et al.*¹⁶ experiment and $\lambda/4\bar{v}_{\text{source}} \sin \theta = 60 \text{ nsec}$ for the Foster *et al.*¹⁷ experiment. Compared with the transit time $w_0/\bar{v}_{\text{source}}$, these numbers move closer to the decay times for the vacuum Rabi oscillation of 94 nsec and 29 nsec, respectively. The distances traveled along the cavity axis in $w_0/\bar{v}_{\text{source}}$ are, respectively, $w_0 \sin \theta = 0.53\lambda$ and $w_0 \sin \theta = 0.28\lambda$. Under these conditions, a detailed accounting for the shape of the correlation function is difficult to give. Broadly speaking, fast atoms produce the central component and short correlation time, while slower atoms are responsible for the long correlation time shown by the background (adiabatic) component. Increasing the tilt of the atomic beam brings about a greater separation between the fast and slow correlation times.

Using simple functional fits we estimate the short correlation time as 40-50 nsec for the Rempe *et al.*¹⁶ experiment [Fig. 4(d)] and 20 nsec for the experiment of Foster *et al.*¹⁷ [Fig. 5(d)]. Consistent numbers are recovered by adding the decay rate of the vacuum Rabi oscillation to the inverse travel time through a quarter wavelength; thus, we obtain $(1/94 + 1/86)^{-1} \text{ nsec} = 45 \text{ nsec}$ and $(1/29 + 1/60)^{-1} \text{ nsec} = 20 \text{ nsec}$, respectively, in good agreement with the correlation times deduced from the figures.

The last and possibly most important feature to note is the oscillation in Fig. 4(d) compared with the monotonic decay in Fig. 5(d). The frequency of oscillation is the vacuum Rabi frequency, which shows clearly that the oscillatory feature is caused by the nonadiabatic response of the photon number to atomic beam density fluctuations. For the chosen atomic beam tilts, the transit time through a quarter wavelength is approximately equal to the decay time of the vacuum Rabi oscillation in the experiment of Rempe *et al.*,¹⁶ while it is twice that in the experiment of Foster *et al.*¹⁷ The Rempe *et al.* experiment is therefore further into the nonadiabatic regime and we suggest that this is the principle reason for its greater degradation of the measured quantum correlations (Fig. 1).

4. SIMULATION RESULTS AND DATA FITS

In this section we present the results of full *ab initio* simulations of the experiments of Rempe *et al.*¹⁶ and Foster *et al.*¹⁷ with the tilt of the atomic beam chosen to optimize the fit to the experimental data. The experiments target the weak-field limit; hence, we initially adopt the two-quanta truncation (4) with the driving field amplitude set to yield a very low rate of photon emission from the cavity (intracavity photon numbers similar to Figs. 2 and 3) and negligible spontaneous emission. Under these conditions, it is impractical to wait for naturally occurring photon emissions. Instead, at regular sample times t_k , emissions from the cavity are forced (see Figs. 2 and 3). Denoting the record with the forced jumps included by $\overline{\text{REC}}$, we compute the intensity correlation function as the ensemble average

$$g^{(2)}(\tau) = \frac{\overline{\langle (\hat{a}^\dagger \hat{a})(t_k) \rangle_{\overline{\text{REC}}} \langle (\hat{a}^\dagger \hat{a})(t_k + \tau) \rangle_{\overline{\text{REC}}} }}{\left(\overline{\langle (\hat{a}^\dagger \hat{a})(t_l) \rangle_{\overline{\text{REC}}} } \right)^2}, \quad (26)$$

where the sample times t_l in the denominator avoid the intervals (a few correlation times) immediately following the jump times t_k ; thus, both ensemble averages are taken in the steady state. The cavity-mode cut-off set at $F = 0.01$, in which case the number of atoms within the interaction volume typically fluctuates around $N(t) \sim 400\text{-}450$ atoms for the Rempe *et al.*¹⁶ experiment and $N(t) \sim 280\text{-}320$ atoms for the Foster *et al.*¹⁷ experiment. Typically, the number of state amplitudes in the two-quanta expansion is 90,000 or 45,000, respectively.

4.1. Weak-field Limit

From a series of simulations for various atomic beam tilts, for each experiment we have selected the result that fits the measured correlation function most closely. The optimum tilts are 9.7 mrad for the experiment of Rempe *et al.*¹⁶ and 9.55 mrad for the Foster *et al.*¹⁷ experiment. The best fits are shown in Fig. 6. For the Foster *et al.*

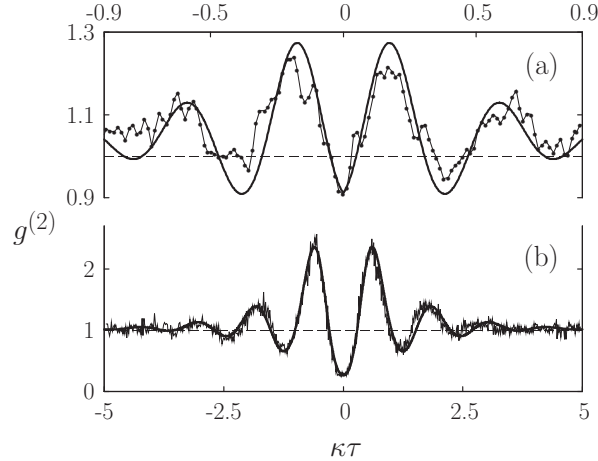


Figure 6. Best fits to the experimental results of Rempe *et al.*¹⁶ (a) and Foster *et al.*¹⁷ (b). The simulations were carried out in the weak-field limit (two-quanta truncation) using the parameters given in Figs. 2 and 3 and atomic beam tilts of 9.7 mrad (a) and 9.55 mrad (b). Ensemble averages of (a) 200,000 and (b) 50,000 samples were taken with a cavity-mode cut-off $F = 0.01$.

*al.*¹⁷ experiment the fit is extremely good. The only obvious disagreement is that the frequency of the vacuum Rabi oscillation is possibly a little low. This, however, would be corrected by a small increase in atomic beam density, the parameter \bar{N}_{eff} , which is only approximately known from the experimental results. The fit to the data of Rempe *et al.*¹⁶ is also good, though certainly not as good as in the previous case. In particular, there is some suggestion that the atomic beam tilt used is a little too large; note how in Fig. 6(a) the depths of the three central minima are almost equal, while the data suggest that the curve should follow the shape of a damped oscillation more closely. The minimum at $\kappa\tau = 0$ is raised relative to those on either side. This is caused by the sharp maximum in the semiclassical correlation function of Fig. 4(d). The trend is accentuated by increased tilt, so that at tilts a little larger than 9.55 mrad the central minimum lies above the other two. The fit of Fig. 6(a) is nonetheless consistent with the data to within the uncertainty set by the shot noise, which introduces error bars of a few percent (see Fig. 8). Thus, leaving aside possible adjustments due to noise sources that are omitted from the simulations (spontaneous emission, atomic and cavity detunings), our results provide strong support for the proposal that the disagreement between theory and experiment presented in Fig. 1 arises from an atomic beam misalignment of approximately 0.5° .

We should make one more observation regarding the atomic beam tilt used in Fig. 6(a). Figure 7(b) replots the best fit for the Rempe *et al.*¹⁶ experiment over a larger range of time delay. For comparison, frame (a) of the figure plots the correlation function obtained from our simulations for a perfectly aligned atomic beam. Aside from the reduced amplitude of the vacuum Rabi oscillation in the presence of the tilt, the correlation function for the 9.7 mrad atomic beam tilt exhibits a broad background due to density fluctuations, which is absent for the aligned atomic beam. The experimental data exhibits just such a background (Fig. 3(a) of Ref. [1]), and an estimate of the long correlation time from Fig. 7(b) yields approximately 400 nsec, consistent with the experimental measurement. It is significant that this number is more than twice the transit time $w_0/\bar{v}_{\text{source}} = 182 \text{ nsec}$.²⁴ The broad background mimics the feature associated with slow atoms in Fig. 4(d) and appears to arise specifically from the discussed separation of adiabatic and nonadiabatic responses to density fluctuations for a tilted atomic beam.

4.2. Intracavity Photon Number and Spontaneous Emission

The fits displayed in Fig. 6 were obtained using a two-quanta truncation of the Hilbert space premised upon the weak-field limit. The strict definition of this limit given in Sec. 2.2 sets a severe constraint on the intracavity photon number. To quantify the constraint we may use Eq. (15) to obtain an estimate of the typical photon

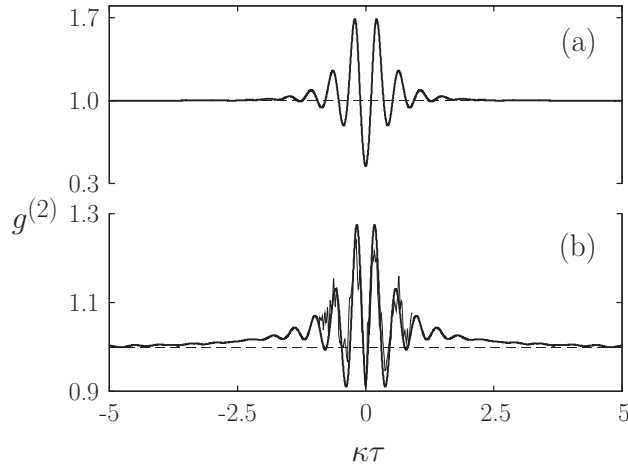


Figure 7. Simulation of the intensity correlation function using the parameters of Rempe *et al.*¹⁶ given in Fig. 2 with no tilt of the atomic beam (a) and an atomic beam tilt of 9.7 mrad (b). Ensemble averages of (a) 15,000 and (b) 200,000 samples were taken with a cavity-mode cut-off $F = 0.01$. The data are plotted with the simulation result in (b).

emission rate from the cavity (into all output channels)

$$R_{\text{cavity}} = 2\kappa \langle (\hat{a}^\dagger \hat{a})(t) \rangle_{\text{REC}} = 2\kappa \left(\frac{\mathcal{E}/\kappa}{1 + 2C_{\{\mathbf{r}_j(t)\}}} \right)^2. \quad (27)$$

Observing then the corresponding estimate of the spontaneous emission rate^{10,12}

$$R_{\text{spon}} = \gamma \sum_{k=1}^{N(t)} \langle (\hat{\sigma}_{k+} \hat{\sigma}_{k-})(t) \rangle = \gamma \sum_{k=1}^{N(t)} \left(\frac{g(\mathbf{r}_k)}{\gamma/2} \frac{\mathcal{E}/\kappa}{1 + 2C_{\{\mathbf{r}_j(t)\}}} \right)^2 = 2C_{\{\mathbf{r}_j\}} 2\kappa \langle (\hat{a}^\dagger \hat{a})(t) \rangle_{\text{REC}}, \quad (28)$$

we arrive at the ratio of spontaneous to cavity emission

$$\frac{R_{\text{spon}}}{R_{\text{cavity}}} = 2C_{\{\mathbf{r}_j\}} = \frac{2N_{\text{eff}}^{\{\mathbf{r}_j\}} g_{\text{max}}^2}{\kappa\gamma} \sim \frac{2\bar{N}_{\text{eff}} g_{\text{max}}^2}{\kappa\gamma}. \quad (29)$$

Now for the two-quanta truncation to be justified, the greater of these emission rates should be much smaller than the inverse of the vacuum Rabi oscillation decay time—i.e., the time for the between-jump evolution to recover the steady state after a photon emission. If this is not so, sequences of three or more quantum jumps can occur too closely spaced in time, thus introducing errors at dominant order in the truncated state. Under the conditions of the experiments, the spontaneous emission rate is the greater by a factor of 70-80; thus, the constraint on intracavity photon number is

$$\langle (\hat{a}^\dagger \hat{a})(t) \rangle \ll \frac{1 + \gamma/2\kappa}{8\bar{N}_{\text{eff}} g_{\text{max}}^2 / \kappa\gamma}. \quad (30)$$

From the numbers given in the captions to Figs. 2 and 3, the right-hand side evaluates as 1.2×10^{-2} for the Rempe *et al.*¹⁶ experiment and 4.7×10^{-3} for the experiment of Foster *et al.*¹⁷; the intracavity photon numbers deduced from the experimental count rates are, respectively, 3.8×10^{-2} and 7.6×10^{-3} . It follows that neither experiment is strictly in the weak-field limit, and it becomes important to ask how spontaneous emission might affect the good agreement in Fig. 6.

In order to address this issue, we have extended our simulations beyond the weak-field limit using a three-quanta truncation of the Hilbert space. To reduce the computational effort, the cavity-mode cut-off is changed

from $F = 0.01$ to $F = 0.1$; thus, the typical number of atoms within the interaction volume is reduced by a factor of approximately two, to $N(t) \sim 180$ -220 atoms for the Rempe *et al.*¹⁶ experiment and $N(t) \sim 150$ -170 atoms for the Foster *et al.*¹⁷ experiment. With the inclusion of the three-quanta states, the number of state amplitudes increases to 1,300,000 and 700,000, respectively. This change to the cavity-mode cut-off introduces minimal error, reducing \bar{N}_{eff} , hence the vacuum Rabi frequency, by only one or two percent.

One more approximation is needed. At the excitation strengths used for the experiments, even a three-quanta truncation has limited validity, since clumps of spontaneous emissions occur that can result in three or more quantum jumps very closely spaced in time. In order to minimize the error introduced by such events, we impose a restriction on the number of quantum jumps permitted within a given time interval. For the three-quanta truncation, the accepted number was set at two and the time interval at $1\kappa^{-1}$ in simulations of the Rempe *et al.*¹⁶ experiment and $3\kappa^{-1}$ in simulations of the Foster *et al.*¹⁷ experiment. With these settings, approximately 10% of the spontaneous emissions were neglected at the highest excitation levels considered.

The results of our three-quanta simulations are presented in Fig. 8, where we have used the optimal atomic beam tilts of Fig. 6. Figure 8(a) compares the simulation with the data of Rempe *et al.*¹⁶ at an intracavity photon number approximately six times smaller than that estimated for the experiment; we are unable to treat the higher number within the three-quanta truncation. The fit overall is as good as that in Fig. 6(a), with a slight improvement in the relative depths of the three minima at the center of the correlation function. A small systematic disagreement does appear to remain, however, and we suspect that the tilt of the atomic beam was in fact a little less, in the experiment, than the 9.7 mrad used, while the contribution of spontaneous emission to the damping of the vacuum Rabi oscillation was a little more. Considering the current numerical limitations, there is little point in searching for a better fit though.

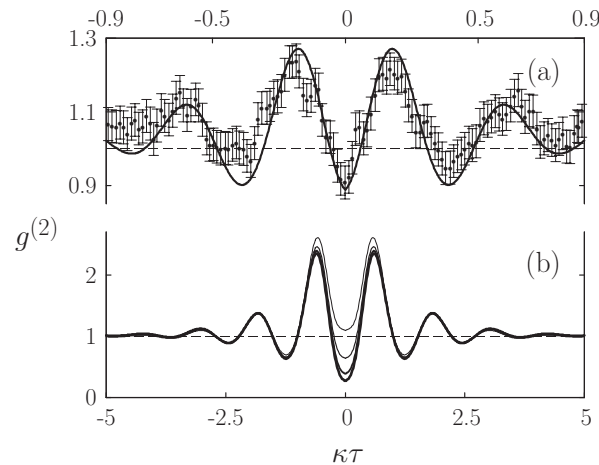


Figure 8. Simulations outside the weak-field limit (three-quanta truncation) for the parameters given in Figs. 2 and 3 of Rempe *et al.*¹⁶ (a) and Foster *et al.*¹⁷ (b); shot noise error bars have been added to the data in (a). Mean intracavity photon numbers are (a) $\langle a^\dagger a \rangle = 6.7 \times 10^{-3}$ and (b) $\langle a^\dagger a \rangle = 2.2 \times 10^{-4}$, 5.7×10^{-4} , 1.1×10^{-3} , and 1.7×10^{-3} (thickest curve to thinnest curve). Ensemble averages of 20,000 samples were taken with a cavity-mode cut-off $F = 0.1$. Atomic beam tilts the same as for Fig. 6.

Figure 8(b) displays results for the parameters of the Foster *et al.*¹⁷ experiment. Four different intracavity photon numbers are considered. For the lowest, $\langle \hat{a}^\dagger \hat{a} \rangle = 2.2 \times 10^{-4}$, the three-quanta truncation closely reproduces the weak-field result of Fig. 6(b). As the photon number is increased, spontaneous emission modifies the correlation function, especially around $\kappa\tau = 0$, where it raises the value of $g^{(2)}(0)$, such that for the largest photon number considered we find $g^{(2)}(0) > 1$. Yet even this largest photon number is smaller, by a factor of five, than the estimate for the experiment. Here, then, we find significant disagreement with the experimental results. The simplest resolution of this disagreement would be for the estimate of the experimental photon number to be too high. On the other hand, a reduction by more than an order of magnitude is needed, and such a large

overestimate seems unlikely considering how the inference from the measured photon count rates is made. At this stage the anomaly remains unresolved.

5. CONCLUSION

We have addressed the disagreement between the weak-field theory of intensity correlations in cavity QED and experimental measurements of the intensity correlation function using thermal atomic beams. A quantum trajectory simulation of the experiments has been developed that includes a Monte-Carlo simulation of the atomic beam and allows for a possible tilt of the beam away from perpendicular to the cavity axis. Two experimental data sets were selected for comparison with the simulations, one from the earliest experiment by Rempe *et al.*¹ and a second from the recent experiment by Foster *et al.*³ Both measurements show disagreements with theory, by overall scale factors of 2 to 4.

We have argued that the disagreement is due to atomic motion and its influence on the quantum correlations through density fluctuations of the atomic beam. The possible role of atomic motion was mentioned in Ref. [1]. We find it more complex, however, than suggested there. In particular, a significant tilt of the atomic beam is needed to bring theory and experiment into agreement. The tilt introduces a component of velocity along the cavity axis, and by way of the resulting motion through the standing wave, a nonadiabatic response of the intracavity photon number to density fluctuations of the atomic beam; thus, classical noise is introduced which degrades the measured quantum correlation.

Working in the weak field limit, *ab initio* simulations of the experiments were performed taking the tilt of the atomic beam as the only adjustable parameter. Excellent agreement was obtained with the experiment of Foster *et al.*¹⁷ for a 9.55mrad tilt, and good agreement with the experiment of Rempe *et al.*¹⁶ using a tilt of 9.7mrad. Background fluctuations in the latter case agree with those seen in the experiment, both in their magnitude and correlation time, and are consistent with our proposed mechanism for the degradation of the quantum correlations.

We found that both experiments operate near, but not strictly in the weak-field limit. Our simulations were therefore extended, subject to numerical constraints, to take spontaneous emission into account. This slightly improved the fit to the data of Rempe *et al.*,¹⁶ and suggested that the optimal fit in this case might be obtained with a somewhat smaller atomic beam tilt and a larger damping of the correlations by spontaneous emission; a more efficient numerical method is needed to pursue the suggestion. Under the conditions of the Foster *et al.*¹⁷ experiment, spontaneous emission was highly detrimental. Even for an intracavity photon number five times smaller than that estimated from the experimental count rates, a large disagreement with the experimental data appeared. No explanation for this anomaly has yet been found.

Problems with atomic motion and the spatial variation of coupling strengths have plagued cavity QED at optical frequencies for many years. As addressed in this paper, nonclassical features of the quantum correlations are predicted at much larger levels than those observed, while other interesting features of the quantum fluctuations remain inaccessible to experiment.²⁵ For some years now, experiments in optical cavity QED have been moving beyond the use of thermal atomic beams to cold and trapped atoms.^{4,26-28} Our method of *ab initio* simulation will be extended to provide a realistic modeling of experiments in this domain as well.

ACKNOWLEDGMENTS

This work was supported by the Marsden Fund of the RSNZ.

REFERENCES

1. G. Rempe, R. J. Thompson, R. J. Brecha, W. D. Lee, and H. J. Kimble, "Optical bistability and photon statistics in cavity quantum electrodynamics," *Phys. Rev. Lett.* **67**, p. 1727, 1991.
2. S. L. Mielke, G. T. Foster, and L. A. Orozco, "Nonclassical intensity correlations in cavity QED," *Phys. Rev. Lett.* **80**, p. 3948, 1998.
3. G. T. Foster, S. L. Mielke, and L. A. Orozco, "Intensity correlations in cavity QED," *Phys. Rev. A* **61**, p. 053821, 2000.

4. K. M. Birnbaum, A. Boca, R. Miller, A. D. Boozer, T. E. Northup, and H. J. Kimble, "Photon blockade in an optical cavity with one trapped atom," *Nature* **436**, p. 87, 2005.
5. G. T. Foster, L. A. Orozco, H. M. Castro-Beltran, and H. J. Carmichael, "Quantum state reduction and conditional time evolution of wave-particle correlations in cavity QED," *Phys. Rev. Lett.* **85**, p. 3149, 2000.
6. G. T. Foster, W. P. Smith, J. E. Reiner, and L. A. Orozco, "Time-dependent electric field fluctuations at the subphoton level," *Phys. Rev. A* **66**, p. 033807, 2002.
7. H. J. Carmichael, G. T. Foster, L. A. Orozco, J. E. Reiner, and P. R. Rice, "Intensity-field correlations of non-classical light," *Progress in Optics* **46**, p. 355, 2004.
8. J. J. Sanchez-Mondragon, N. B. Narozhny, and J. H. Eberly, "Theory of spontaneous-emission line shape in an ideal cavity," *Phys. Rev. Lett.* **51**, p. 550, 1983.
9. G. S. Agarwal, "Vacuum-field Rabi splittings in microwave absorption by Rydberg atoms in a cavity," *Phys. Rev. Lett.* **53**, p. 1732, 1984.
10. H. J. Carmichael, R. Brecha, and P. R. Rice, "Quantum interference and collapse of the wavefunction in cavity QED," *Opt. Comm.* **82**, p. 73, 1991.
11. L. Tian and H. J. Carmichael, "Quantum trajectory simulations of two-state behavior in an optical cavity containing one atom," *Phys. Rev. A* **46**, p. R6801, 1992.
12. R. J. Brecha, P. R. Rice, and M. Xiao, "N two-level atoms in a driven optical cavity: Quantum dynamics of forward photon scattering for weak incident fields," *Phys. Rev. A* **59**, p. 2392, 1999.
13. H. J. Carmichael, H. M. Castro-Beltran, G. T. Foster, and L. A. Orozco, "Giant violations of classical inequalities through the conditional homodyne detection of the quadrature amplitudes of light," *Phys. Rev. Lett.* **85**, p. 1855, 2000.
14. Martini and Schenzle made a theoretical fit to a data set from Ref. [1] by numerically solving a many-atom master equation for equal coupling strengths.²⁹ The calculations are taken outside the weak-field limit and good agreement with the experiment is shown. The parameters used are very far from the experimental ones, though, with the dipole coupling strength smaller by a factor of approximately three.
15. H. J. Carmichael and B. C. Sanders, "Multiatom effects in cavity QED with atomic beams," *Phys. Rev. A* **60**, p. 2497, 1999.
16. Figure 4(a) of Ref. [1].
17. Figure 4 of Ref. [3].
18. H. J. Carmichael, "Photon antibunching and squeezing for a single atom in a resonant cavity," *Phys. Rev. Lett.* **55**, p. 2790, 1985.
19. P. R. Rice and H. J. Carmichael, "Single-atom cavity-enhanced absorption I: Photon statistics in the bad-cavity limit," *IEEE J. Quantum Electron.* **24**, p. 1351, 1988.
20. Previous fits to the experimental measurements were made by taking ensemble averages of the normalized correlation function (5).^{1,3} In fact the normalization is given correctly in Eq. (11). When defined in this way, $g^{(2)}(\tau)$ is not asymptotic to $g^{(2)}(\infty) = 1$; but this is to be expected, as the atomic beam fluctuations have infinite correlation time when the atomic motion is neglected.
21. H. J. Carmichael, *An Open Systems Approach to Quantum Optics, Lecture Notes in Physics, Vol. m18*, Springer-Verlag, Berlin, 1993.
22. J. Dalibard, Y. Castin, and K. Mølmer, "Wave-function approach to dissipative processes in quantum optics," *Phys. Rev. Lett.* **68**, p. 127902, 2004.
23. L.-M. Dum, P. J. Zoller, and H. Ritsch, "Monte-carlo simulation of the atomic master equation for spontaneous emission," *Phys. Rev. A* **45**, p. 4879, 1992.
24. A correlation time for the background of 400nsec is consistent with the transit time if the latter is defined as $2w_0/\bar{v}_{\text{source}} = 364\text{nsec}$, or using the peak rather than the average velocity, as $4w_0/\sqrt{\pi}\bar{v}_{\text{source}} = 411\text{nsec}$.¹ We have assumed that the time to replace an ensemble of interacting atoms with a statistically independent one is closer to $w_0/\bar{v}_{\text{source}}$, which is the number suggested by the semiclassical correlation functions in Figs. 4 and 5.
25. P. Alsing and H. J. Carmichael, "Spontaneous dressed-state polarization of a coupled atom and cavity mode," *Quant. Opt.* **3**, p. 13, 1991.

26. C. J. Hood, T. W. Lynn, A. C. Doherty, A. S. Parkins, and H. J. Kimble, "The atom-cavity microscope: single atoms bound in orbit by single photons," *Science* **287**, p. 1447, 2000.
27. P. W. H. Pinsky, T. Fischer, P. Maunz, and G. Rempe, "Trapping an atom with single photons," *Nature* **404**, p. 365, 2000.
28. M. Hennrich, A. Kuhn, and G. Rempe, "Transition from antibunching to bunching in cavity QED," *Phys. Rev. Lett.* **94**, p. 053604, 2005.
29. U. Martini and A. Schenzle, "Cavity QED with many atoms," in *Directions in Quantum Optics*, H. J. Carmichael, R. J. Glauber, and M. O. Scully, eds., *Lecture Notes in Physics*, pp. 238–249, Springer, (Berlin), 2001.